



THE UNIVERSITY *of* EDINBURGH

Edinburgh Research Explorer

A nickel-complex sensitiser for dye-sensitised solar cells

Citation for published version:

Linfoot, CL, Richardson, P, McCall, KL, Durrant, JR, Morandeira, A & Robertson, N 2011, 'A nickel-complex sensitiser for dye-sensitised solar cells' *Solar energy*, vol. 85, no. 6, pp. 1195-1203. DOI: 10.1016/j.solener.2011.02.023

Digital Object Identifier (DOI):

[10.1016/j.solener.2011.02.023](https://doi.org/10.1016/j.solener.2011.02.023)

Link:

[Link to publication record in Edinburgh Research Explorer](#)

Document Version:

Peer reviewed version

Published In:

Solar energy

Publisher Rights Statement:

Copyright © 2011 Elsevier Ltd. All rights reserved.

General rights

Copyright for the publications made accessible via the Edinburgh Research Explorer is retained by the author(s) and / or other copyright owners and it is a condition of accessing these publications that users recognise and abide by the legal requirements associated with these rights.

Take down policy

The University of Edinburgh has made every reasonable effort to ensure that Edinburgh Research Explorer content complies with UK legislation. If you believe that the public display of this file breaches copyright please contact openaccess@ed.ac.uk providing details, and we will remove access to the work immediately and investigate your claim.



This is the peer-reviewed author's version of a work that was accepted for publication in *Solar energy*. Changes resulting from the publishing process, such as editing, corrections, structural formatting, and other quality control mechanisms may not be reflected in this document. Changes may have been made to this work since it was submitted for publication. A definitive version is available at: <http://dx.doi.org/10.1016/j.solener.2011.02.023>

Cite as:

Linfoot, C. L., Richardson, P., McCall, K. L., Durrant, J. R., Morandeira, A., & Robertson, N. (2011). A nickel-complex sensitiser for dye-sensitised solar cells. *Solar energy*, 85(6), 1195-1203.

Manuscript received: 30/10/2009; Accepted: 26/02/2011; Article published: 24/03/2011

A nickel-complex sensitiser for dye-sensitised solar cells**

Charlotte L. Linfoot,¹ Patricia Richardson,¹ Keri L. McCall,¹ James R. Durrant,² Ana Morandeira²
and Neil Robertson^{1,*}

^[1]EaStCHEM, School of Chemistry, Joseph Black Building, University of Edinburgh, West Mains Road, Edinburgh, EH9 3JJ, UK.

^[2]Centre for Electronic Materials and Devices, Department of Chemistry, Imperial College London, London SW7 2AZ, UK.

^[*]Corresponding author; e-mail: neil.robertson@ed.ac.uk

^[**]We thank EaStChem for studentship funding (CLL) and the EPSRC Supergen programme for further financial support. This work has made use of the resources provided by the EaStCHEM Research Computing Facility, partially supported by the eDIKT initiative.

Keywords

Dye-Sensitised Solar Cell; Nickel complex; Photoelectrochemical; DFT; TD-DFT; Sensitizer

Abstract

We report the first example of a Ni(II) complex that demonstrates sensitiser function in a Dye-Sensitised Solar Cell (DSSC). Complexes [Ni(dcbpy)(qdt)] (**1**), [Ni(decby)(qdt)] (**2**) and [Ni(decby)Cl₂] (**3**) (where; dcbpy = 4,4'-dicarboxy-2,2'-bipyridine; decby = 4,4'-di(CO₂Et)-2,2'-bipyridine; and qdt = quinoxaline-2,3-dithiolate) have been prepared. Characterisation was carried out using electrochemical, spectroscopic and computational techniques. Intensive visible transitions of **1** and **2** have been assigned predominantly to Ligand-to-Ligand Charge Transfer (LLCT) from the qdt to the diimine ligand, suggesting appropriate charge separation for application in a photoelectrochemical device. TiO₂ sensitised with **2**, following charge injection, processes a recombination time significantly long for photovoltaic function. In a DSSC, using I⁻/I₃⁻ redox electrolyte, photocurrents and photovoltages of 0.293 mA and 521 mV were observed, with optimum values requiring TiCl₄ post-treatment of TiO₂ and co-adsorption of Chenodeoxycholic acid (Cheno). Although photovoltaic function was observed, the low photocurrent is attributed to a short-lived excited state lifetime resulting in poor charge injection from the Ni(II) sensitiser.

1. Introduction

Improving alternative energy sources capable of meeting the global demand has recently been rekindled as the modern world faces up to the ever increasing problem of global warming (Eisenberg, 2005; Zweible, 1993). Renewable, carbon-neutral energy sources are the future, with one of the fore-runners being solar energy. In 1991, O'Regan and Grätzel devised a new generation of solar cell, the Dye-Sensitised Solar Cell (DSSC).

DSSC's comprise five main elements; the Transparent-Conducting-Oxide Electrode (TCO), the metal oxide semiconducting electrode (most commonly TiO₂), the sensitiser dye molecule, the hole transport material (HTM) and the Platinum electrode (Robertson, 2006). The sensitiser acts as a photodriven molecular electron pump; harvesting sunlight and injecting the excited electrons into the semiconductor. The sensitiser molecule is then re-reduced by the HTM. Sensitiser molecules are therefore designed so that their D*/D⁺ and D/D⁺ energy levels allow successful charge injection into TiO₂, and dye regeneration by the HTM. The photovoltaic processes that need to be maximised are the light harvesting efficiency (LHE) in the visible region, generation of efficient charge separation, and biasing the forward electron transfer rates over the reverse (Gregg, 2004). This last factor is achieved by sensitizing the wide band-gap semiconductors using molecular sensitisers designed to allow control of the interfacial and intercomponent electron transfer process kinetics (Bignozzi *et al.*, 2000). The final design consideration is that the sensitiser must form a monolayer over the TiO₂ and therefore must contain some anchoring group. The most successful anchoring groups found to date are carboxyl groups which form ester linkages with the metal oxide (Zakeerudin *et al.*, 1997). In this work, the carboxyl groups were located as substituents groups on the bipyridine ligand.

To date DSSCs have been constructed using a range of transition metal complexes; Ru(II), Os(II), Pt(II), Re(I), Cu(I), Fe(II) (Robertson, 2006). The most successful cells contain Ru(II) sensitizer molecules, some of which are being commercially developed for niche markets. However, there are downsides to using Ru(II), firstly low abundance, and secondly toxicity considerations which could both present practical implications in the long term. Research into DSSCs has therefore extended to exploring the possibilities of first row transition metals. Research into this field however, has been limited due to their extremely short-lived excited states compared to 2nd and 3rd row transition metal complexes. It is known that crossing from the charge-transfer excited state to a d-d excited state leads to a short lived excited state lifetime. For first row transition metals the charge-transfer and d-d excited states are very close in energy, making crossing, and therefore non-radiative decay from the excited state, favourable. The result is that charge injection into the TiO₂ becomes the limiting factor, as the excited state is not long lived enough.

Two sensitizer design strategies have been implemented to try and overcome this problem for first row transition metal coordination complexes. The first is to have complexes with a full d-subshell and, the second to have a strong crystal field, aimed at raising the energy of any d-d excited states. Both these result in a longer lived excited state compared to other first row transition metals (Robertson, 2008).

Cu(I) is under investigation as a DSSC sensitizer, taking advantage of its d¹⁰ configuration allowing the excited state to be longer lived. Cu(I) sensitizers can obtain overall cell efficiencies in some cases ranging to over 2% (Abonso-Vante *et al.*, 1994; Sakai *et al.*, 2002; Bessho *et al.*, 2008; Constable *et al.*, 2009).

Ferrere *et al.*, (1998; 2000; 2002) based their design of Fe(II) sensitizer molecules around obtaining a strong crystal field. They took their lead from successful, analogous Ru(II) sensitizers that exhibit strong crystal-field splitting (Nazeeruddin *et al.*, 1993). The aim was that the excited state lifetime of the Fe(II) sensitizers would be long lived enough to allow sufficient charge injection into TiO₂. Solar cell function was observed but it was significantly reduced compared to the analogous Ru(II) sensitizer leading to no subsequent reports of research into Fe(II).

Research presented here investigates the possible use of Ni(II) complexes as sensitizer molecules. Ni(II) preferentially forms square planar complexes, which characteristically exhibit strong crystal fields. Based on the design rationale outlined above it was hoped that a strong crystal field would lead to increased charge injection into TiO₂. The design of the Ni(II) sensitizer synthesised during this work was based upon previous Pt(II) research (Geary *et al.*, 2005; Islam *et al.*, 2001) and reports the first example of a [Ni(II)(bpy)(qdt)] complex that has been synthesised and subsequently spectroscopically and electronically characterised. This is also the first time a Ni(II) complex has been reported to show DSSC function.

2. Results and Discussion

2.1. Syntheses

The ligands 4,4'-dicarboxy-2,2'-bipyridine (dcbpy), 4,4'-di(CO₂Et)-2,2'-bipyridine (decbpy) and 2,3-quinoxalinedithiol (qdt) were synthesised using modified literature method as described in the Experimental details. The Ni(II) complexes synthesised during this work as shown in Figure 1, which also outlines the reaction scheme. All complexes were synthesised by simple addition, with stirring, of the relevant starting materials in stoichiometric amounts, to the appropriate solvent at room temperature. The ester analogue (**2**) has been synthesised alongside the acid (**1**), despite not being directly applicable for use in a DSSC, as the properties of ester are known to be similar to the acid, and are more convenient for detailed characterisation due to better solubility. The Ni(II) complexes were characterised by ¹H NMR, ESI-MS, +FAB-MS and elemental analysis verifying the molecular structures. The electrochemical and photophysical properties of the complexes and the qdt ligand were investigated using UV/Vis spectroscopy, electrochemistry and emission spectroscopic studies. [Ni(decbpy)Cl₂] (**3**) was synthesised to facilitate assignment of the electrochemical and spectroscopic properties of **1** and **2**. Solar cell function of **1** was investigated using *I-V* characterisation and Transient Absorption Decay studies. Density Functional Theory (DFT) and Time-Dependant DFT (TD-DFT) calculations were used to support and further investigate these properties.

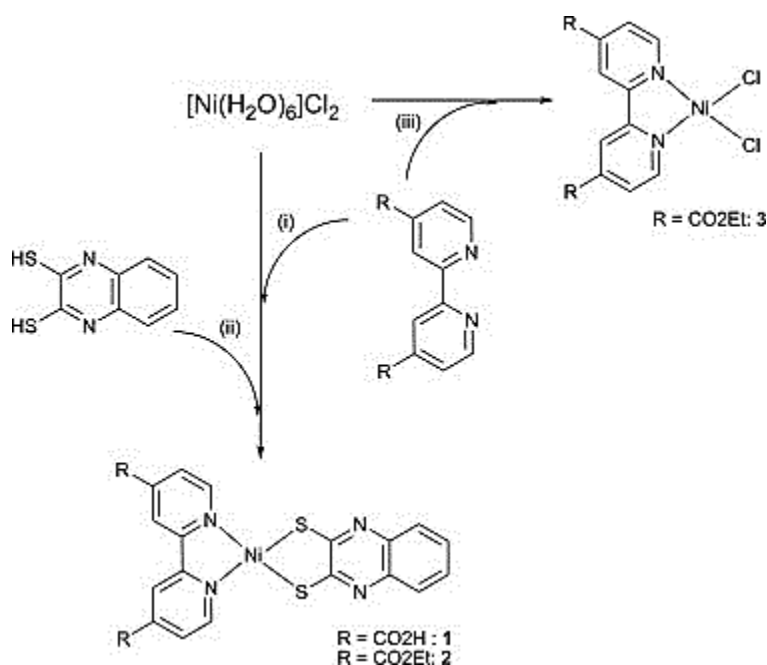


Figure 1. Synthetic Reaction Scheme for Complexes reported in this work. (i) R = CO₂H: EtOH and 2eq. NaOH; R= CO₂Et: DCM (ii) EtOH and 2 eq. NaOH: (iii) THF.

2.2. Electrochemistry

The redox potentials of complexes **1** and **2** are shown in Table 1. Given for comparison are the redox potentials for **3**, qdt and the Pt analogue (Islam *et al.*, 2001). As outlined in the introduction, the discussion will focus on the data collected for **2** due to the poorer solubility of **1** and typically less-well-defined reduction processes for such carboxylic-acid substituted complexes.

Reduction of **2** occurs at two potentials; -1.23 V and -0.72 V that can be assigned as being bpy-based reductions upon comparison with **3**. This is consistent with bpy-based reduction potentials quoted in the literature for co-ordination complexes (Armaroli *et al.*, 2001). Both these processes have oxidation-reduction peak separations indicating electrochemical reversibility, although the second reduction has limited chemical reversibility. The multiple oxidations observed for **2** have been assigned as qdt-based by comparison with the oxidation potentials seen for both free qdt and the Pt complex. This is supported by the lack of any oxidation peaks for **3**. This demonstrates that the first oxidation is suitably located for a DSSC sensitiser. Oxidation takes place on the dithiolate and reduction on the diimine, therefore implying that charge transfer transitions across the molecule will likely have directionality towards the carboxylate groups that bind to TiO₂. The location of the HOMO also means that when the sensitiser is oxidised the positive charge density is placed further from the TiO₂. Charge recombination from the TiO₂ back to the dye is expected to be minimised by this physical separation. In addition the similarity of the reduction potential for the Ni(II) complex with the Pt(II) complex suggests that the LUMO of **1** is at an energy suitable to allow charge injection into the TiO₂ conduction band; band edge at -0.81 V vs. Ag/AgCl (Nazeeruddin *et al.*, 1993).

Table 1. Oxidation and Reduction Potentials for; **1**, **2** and qdt in solutions of 0.1M TBABF₄/DMF; **3** in 0.3M TBABF₄/DCM; and [Pt(decbpy)(qdt)](Islam *et al.*, 2001). All potentials vs. Ag/AgCl; recorded at 298K; a = Peaks are electrochemically reversible and values shown represent E_{1/2}; b = Peaks are electrochemically irreversible and values shown represent peak potential.

Sensitiser	E _{1/2} (V vs. Ag/AgCl)			
	E _{Red.2}	E _{Red. 1}	E _{Ox.1}	E _{Ox.2}
[Ni(dcbpy)(qdt)]; 1	-1.17 ^a		0.53 ^a	1.15 ^a
[Ni(decbpy)(qdt)]; 2	-1.23 ^a	-0.72 ^a	0.86 ^b	1.08 ^b
[Ni(decbpy)Cl ₂]; 3	-1.36 ^b	-0.81 ^b		
qdt	-1.12 ^b			1.12 ^b
[Pt(decbpy)(qdt)]	-1.06 ^b		0.90 ^b	

2.3. UV/Vis Absorption Spectroscopy

As can be seen from Table 2 and Figure 2, **2** absorbs in the visible region between 530nm and 560nm.

Assignment of Ligand to Ligand Charge Transfer (LLCT) has been proposed based upon comparison with the

Pt(II) analogues (Geary *et al.*, 2005; Islam *et al.*, 2001) and the TD-DFT calculations (see Section 2.7). The assignment was also supported by comparison with the absorption data collected for **3** and the free qdt ligand. It can clearly be seen that **3** does not undergo low-energy metal to ligand charge transfer (MLCT) or LLCT by the lack of an absorption peak above 400nm. This assignment of LLCT at 533 and 561 nm for **2** is further confirmed by the lack of absorptions above 459 nm for the non-complexed qdt.

A visible absorption at this wavelength and of this magnitude ($\lambda_{\text{max}} = 533 - 561 \text{ nm}$, and $\epsilon = 7.3 \text{ M}^{-1}\text{cm}^{-1} \times 10^3$ respectively) is well within the acceptable range required for a DSSC sensitiser and importantly the region of absorption is red-shifted compared to the analogous Pt(II) sensitiser, and has an increased molar extinction coefficient for this charge transfer (Table 2.).

Table 2. Absorbance measurements for **1**, **2** and qdt carried out in DMF; **3** carried out in DCM; [Pt(decby)(qdt)] in 4:1 EtOH:MeOH solution (Islam *et al.*, 2001).

Complex	Absorption (nm) ($\epsilon / \text{M}^{-1}\text{cm}^{-1} \times 10^3$)		
	$\pi-\pi^*$ intra-bpy	$\pi-\pi^*$ intra-qdt	LLCT
[Ni(dcbpy)(qdt)]; 1	315	424, 445	534, 561
[Ni(decby)(qdt)]; 2	316 (29.0)	410 (2.9)	533 (7.3), 561 (7.3)
[Ni(decby)Cl ₂]; 3	323 (13.3)		
qdt		409 (18.9), 432 (19.1) 459 (11.3)	
[Pt(decby)(qdt)]	305 (13.4)	425 (11.4) 460 (10.3)	495 (5.3)

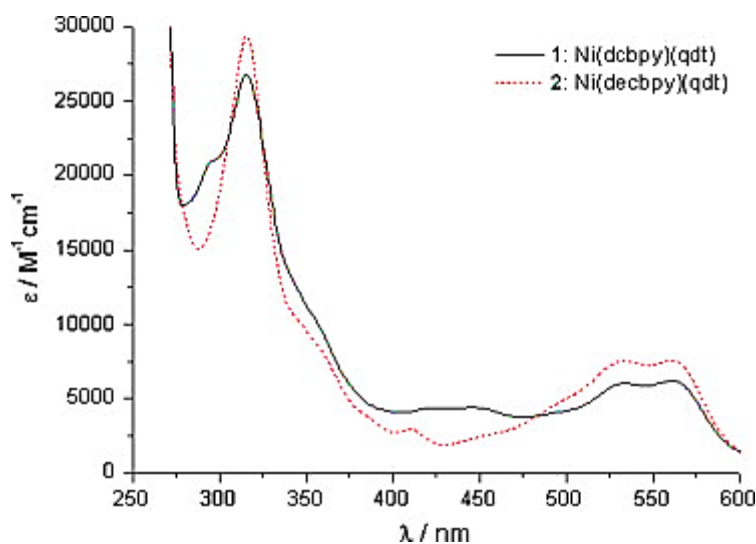


Figure 2. Absorbance Spectra for **1** and **2**. Y axis refers to results for **2**. Spectrum shown for **1** is normalised against **2** as accurate molar extinction coefficients could not be calculated for **1** due to poor solubility.

2.4. Transient absorption decay studies

Transient absorption spectroscopy was used to investigate the electron-transfer kinetics of the dye-sensitised TiO₂ system. Sensitisation of the TiO₂ was achieved by treating a freshly prepared TiO₂ film with pH 12 NaOH (aq) solution for 1 h, and then removing and drying the film (110°C, 5 minutes). The film was then placed into a dye bath (a solution of **2** in DCM), and left for 48 h before removal and air drying. The excitation wavelength was set at 520 nm, previously identified as the light harvesting absorption. Photoinduced absorption was monitored at a probe wavelength of 995 nm, and assigned primarily to absorption electrons injected into the TiO₂ conduction band/trap states.

Figure 3 illustrates that the Ni(II) sensitizer does inject electrons into the conduction band of TiO₂ upon excitation at 520nm. The half time recorded for the electron recombination with the sensitizer was around 0.01 s which is comparable with other effective sensitizers. A recombination time of this length indicates that this loss mechanism is not a limiting factor in this system and is consistent with the assignment of significant charge separation in the LLCT excited state.

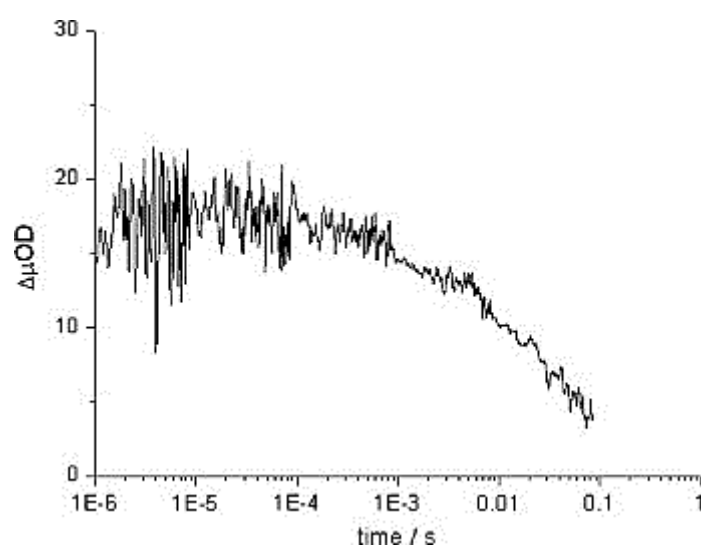


Figure 3. Transient Absorption Decay Trace for [Ni(qdt)(dcbpy)] adsorbed on TiO₂; Excitation wavelength = 520 nm; Probe = 995 nm.

2.5. Solar Cell Measurements

I-V characterisation was carried out on solar cells made using **1** adsorbed onto the TiO₂ film. Cell construction and treatments are outlined in the Experimental section. Overall cell efficiency was determined via *I-V*

characterisation while irradiating under AM 1.5 light (100 mWcm^{-1}). Cell efficiencies (η) were calculated using the resulting values of I_{sc} = short circuit current (mA), V_{oc} = open circuit voltage (mV) and ff = fill factor.

In order to obtain the optimum coverage of the TiO_2 surface with our Ni(II) sensitiser, adsorption studies were carried out. A range of dye bath solvents and dye concentrations were explored, with a 2mM complex in MeCN/t-butanol dye bath yielding the best TiO_2 coverage by our dye. Determination of TiO_2 surface coverage was carried out in an approximate fashion using UV/Vis spectroscopy. This method also allowed confirmation that the dye bound without degradation by comparison with the absorption spectrum of **1** in solution.

The planar geometry of complex **1** suggests that aggregation of the molecule may occur through π - π stacking as Islam *et al.*, found for their Pt(II) complexes in 2001. In a DSSC, dye aggregation can be a significant hindrance as it can limit the number of sensitiser molecules bound to the TiO_2 surface, and may also lead to intermolecular quenching (Ito *et al.*, 2008). Here we have investigated a method outlined in the literature implemented to reduce dye aggregation, involving the use of an additive in the dye bath that acts as a spacer group on the TiO_2 surface. The additive investigated in this work was Chenodeoxycholate acid (Cheno) as it has been shown to dramatically improve the short circuit currents produced in some systems (Chen *et al.*, 2007; Choi *et al.*, 2007; Ito *et al.*, 2008; Sayama *et al.*, 2003; Yum *et al.*, 2008). A range of dye:Cheno concentration ratios were tried for **1** with representative examples shown in Table 3 and Figure 4. Improved solar cell function for the dye:Cheno cells over the non-Cheno cells was observed in every case, although further increase in the quantity of cheno beyond 1 mM led to no further improvement. The Cheno is believed to bind preferentially to TiO_2 over the dye sensitiser, forming a co-adsorption of the two species on the surface. Once enough Cheno is present to prevent aggregation no further benefit is obtained from having excess quantities.

A TiCl_4 post-treatment of the TiO_2 film prior to adsorption of the sensitiser has been discussed widely in the literature as a method of improving photocurrents obtained from a DSSC (Ito *et al.*, 2005; Nazeeruddin *et al.*, 1993). When the TiCl_4 post-treatment was introduced in our work alongside the use of the Cheno-additive, the DSSC function of **1** improves dramatically (Figure 5). The photocurrent produced by **1** doubles (0.122 mA to 0.293 mA respectively). This is consistent with the mode of action described by Sommeling *et al.* in 2006. It was proposed that the TiCl_4 post-treatment acts to improve dye adsorption onto TiO_2 , but that it more importantly increases charge injection into the TiO_2 by causing a downward shift in the conduction band edge of the TiO_2 . There were concerns that a downward shift of the TiO_2 conduction band edge may reduce the V_{oc} produced by the cell. As can be seen in Table 3 and Figure 5, V_{oc} increases by 50mV compared to a non- TiCl_4 post-treated cell which had the same dye:Cheno ratio. It is believed by Sommeling *et al.* (2006) that the increased charge injection caused by the TiCl_4 creates a greater charge density build up in the TiO_2 , therefore maintaining, and perhaps even improving the V_{oc} of the cell.

In order to compare our results with those of the Pt(II) analogue (Islam *et al.*, 2001) it should be taken into account that the Pt(II) cells had an active area of 0.25cm² whereas our cells had an active area of 1cm². A reduced active area is known to produce higher cell efficiencies due to an increase in fill factor. Taking this into account our cells produce V_{oc} potentials that are similar to those of the Pt(II) sensitiser but the photocurrents produced by our Ni(II) sensitiser are significantly reduced. Even with the inclusion of the TiCl₄ post-treatment the photocurrents produced by the Pt(II) sensitiser are around twenty times greater than those produced by the Ni(II) sensitiser (0.293mA and 7.000mA respectively).

Table 3. *IV* Characterisation Data for **1**. Dye bath 2mM MeCN/t-butanol. Adsorption time 24 h. [Pt(qdt)(dcbpy)] 0.05mM in an ethanol dye bath. (Islam *et al.*, 2001).

Sensitiser	Concentration of Cheno	TiCl ₄ treated	Isc / mA	Voc / mV	ff	η (%)
1	N/A	No	0.090	389	0.41	0.006
1	1mM	No	0.172	485	0.52	0.043
1	50mM	No	0.122	476	0.54	0.031
1	50mM	Yes	0.293	521	0.55	0.084
[Pt(dcbpy)(qdt)]: 0.05mM	30mmol	No	7.00	600	0.77	3.000

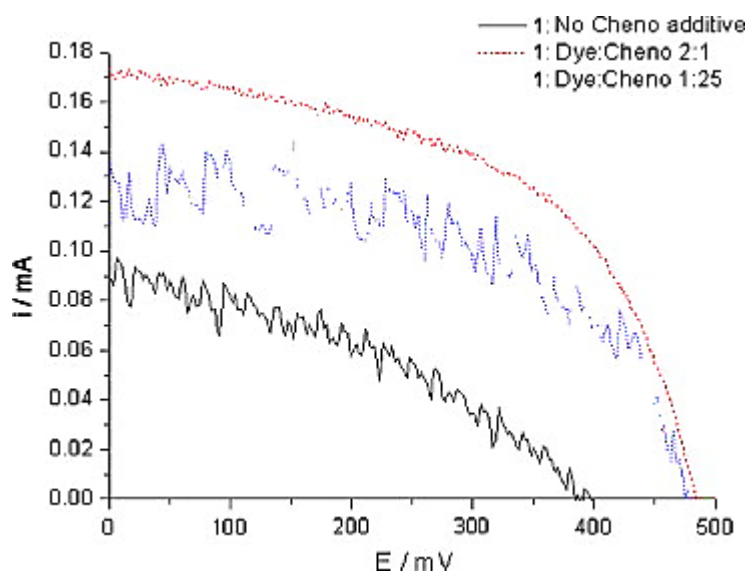


Figure 4. *I-V* Curve for **1**. Black solid line = no Cheno additive; red dashed line = Dye:Cheno 2:1; Blue dotted line = Dye:Cheno 1:25

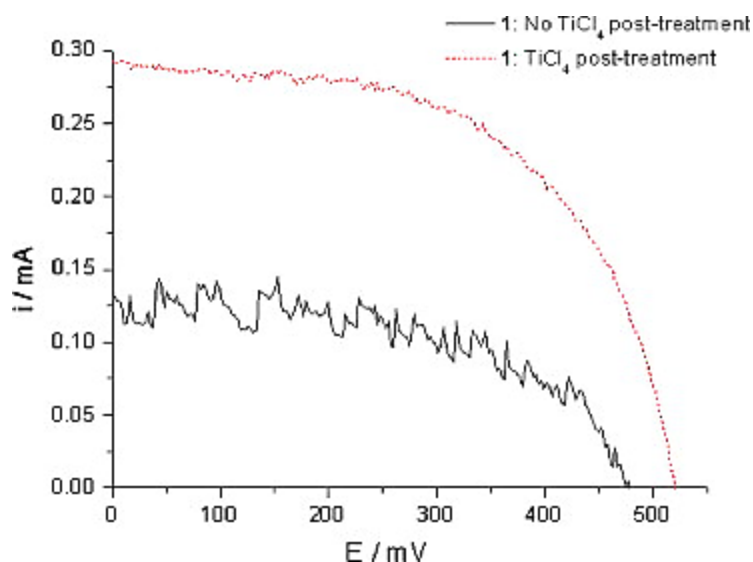


Figure 5. *I-V* Curve for **1**. Dye:Cheno = 1:25. Black line = no TiCl_4 Post-Treatment; red dashed line = TiCl_4 post-treatment.

2.6. Emission

In order to rationalise our solar cell measurements, and in particular the I_{sc} values recorded we investigated the emissive properties of **2**. These studies were carried out to give an indication of the excited state lifetimes of these Ni(II) complexes. Measurements were taken in an ethanolic solution of **2**, and for comparison an ethanolic solution of free qdt ligand. Both solutions emitted very weakly at room temperature upon excitation between 350 and 500 nm. They were non-emissive when exciting at 550nm, this is of note as this is where the LLCT is believed to take place. As the solutions are non-emissive when excited at the LLCT energy, we propose that non-radiative decay pathways are competing with any emissive pathways suggesting the excited lifetime is likely to be short.

2.7. DFT calculations

Gaussian 03 (Frisch *et al.*, 2004) was used to run all the Density Functional Theory (DFT calculations) carried out for this work. We used the Becke three parameters hybrid exchange and the Perdew–Wang 1991 correlation functionals (B3PW91) (Perdew *et al.*, 1993; Perdew *et al.*, 1996). Calculations were performed for complex **1** in a DMF polarisable continuum model (Boes *et al.*, 2006).

The calculated HOMO and LUMO locations can be seen in Figure 6 and the orbital contributions from component parts of the molecule are listed in Table 4. From these percentages we can conclude that the HOMO, although mainly qdt-based, does have a considerable contribution from the Ni(II). The LUMO, as

predicted, is almost entirely bpy based. This is consistent with the HOMO/LUMO locations calculated for the analogous Pt(II) sensitisers (Geary *et al.*, 2005; Islam *et al.*, 2001).

Time-dependent density functional theory (TD-DFT) calculations for **1** were also carried out in a DMF polarisable continuum model (Boes *et al.*, 2006), with the first 70 singlet transitions calculated. TD-DFT calculations allowed a theoretical absorption spectrum for **1** to be generated, and to identify which molecular orbital levels are involved in the charge transitions occurring between 500 and 600 nm. Figure 7 shows the theoretical absorption spectrum for **1** against the standardised experimental spectrum for **1**. The fit between experimental and computational data is comparable with prior studies on transition metal complexes (McCall *et al.*, 2009). The theoretical spectrum shows absorptions at reasonable energies, which, coupled with the calculated molecular orbitals involved in these low energy transitions (Table 5), allows us to propose that the absorptions between 500 and 600 nm are largely the result of LLCT from the qdt-based HOMO, to the bpy-based LUMO.

Table 4. DFT Calculations for the Atomic Orbital Contributions to the HOMO and LUMO levels for **1**.

MO	% Contribution from Ni based MOs	% Contribution from qdt-based MOs	% Contribution from bpy-based MOs
LUMO+4	36.90	33.25	29.85
LUMO+3	1.26	93.98	4.76
LUMO+2	0.04	3.07	96.89
LUMO+1	1.76	0.30	97.94
LUMO	5.91	3.09	91.00
HOMO	24.41	68.80	7.79
HOMO-1	32.75	63.89	3.36
HOMO-2	90.24	3.94	5.82

Table 5. Selected TD-DFT calculated UV/Vis absorptions showing the dominant charge transfer state contributions.

Absorbance λ / nm	Main Charge Transitions		Relative Contribution
	MO from	MO to	
588	HOMO-2	LUMO	32 %
	HOMO-2	LUMO+4	16%
	HOMO-1	LUMO	28 %
	HOMO	LUMO	24 %
582	HOMO-2	LUMO	20 %
	HOMO-2	LUMO+4	19 %
	HOMO-1	LUMO	32 %
	HOMO	LUMO	29 %
569	HOMO-2	LUMO	51 %
	HOMO	LUMO	49 %
433	HOMO	LUMO+1	100 %
411	HOMO-1	LUMO+1	57 %

The computational results are consistent with the observed electrochemical and spectroscopic data, and also the transient absorption decay studies which demonstrates charge injection from [Ni(dcbpy)(qdt)] into TiO₂ with a recombination half time of around 0.01 s. Thus the molecular design determines that charge recombination is not a limiting factor for this dye/semiconductor system presumably due to LLCT placing the positive charge density away from the TiO₂.

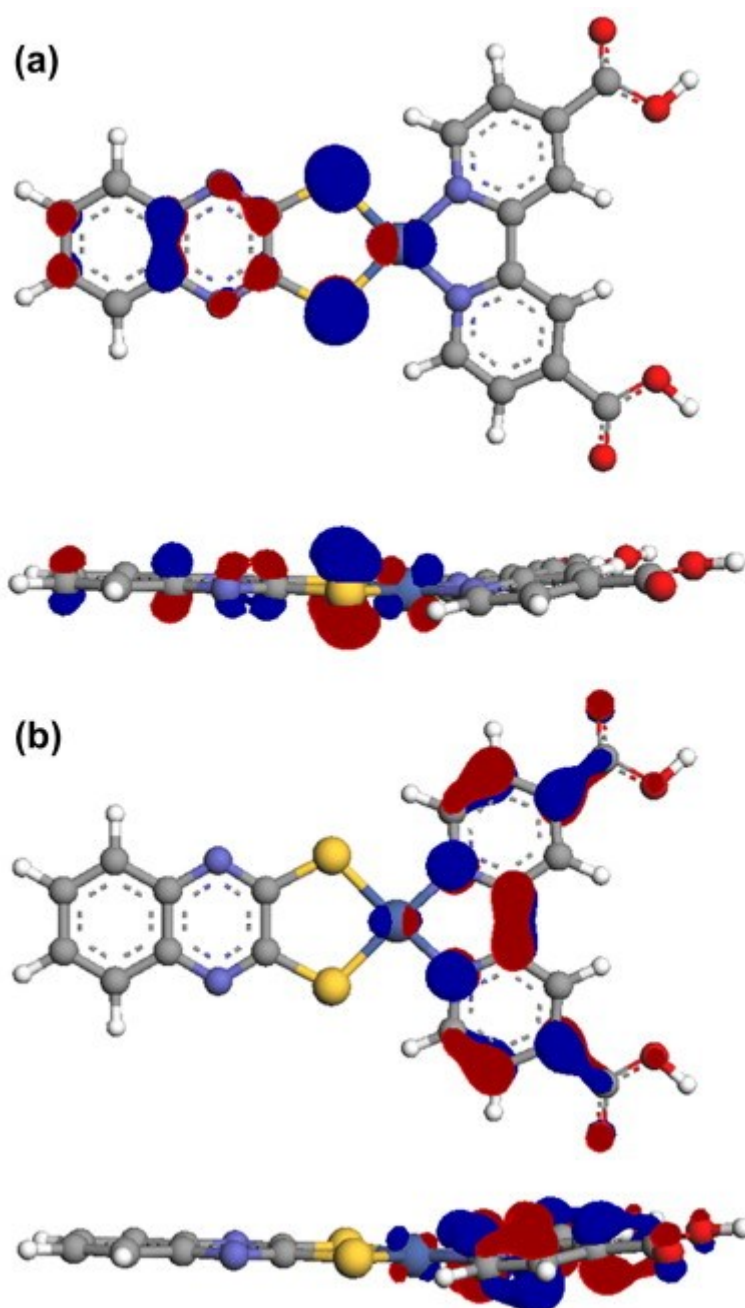


Figure 6. DFT Calculated Geometry Optimisation for 1 including (a) HOMO and (b) LUMO Isosurfaces.

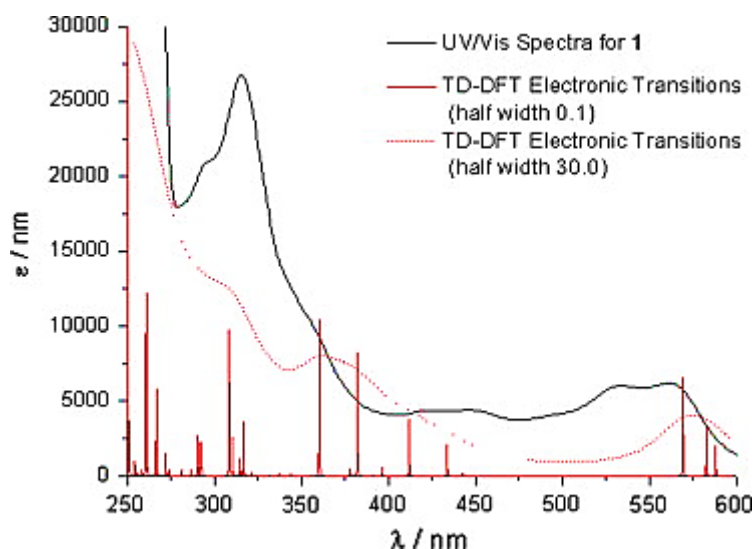


Figure 7. UV/Vis Absorption Spectra; red solid lines = TD-DFT spectrum half width 0.1; red dotted line = TD-DFT spectrum half width 30.0; black dashed line = standardised solution spectrum of **1** in DMF.

3. Conclusions

Shown here is the synthesis of the first example of a Ni(II)(diimine)(dithiolate) with an acid substituents attached to the diimine: [Ni(4,4'-dicarboxy-2,2'-dipyridyl)(2,3-quinoxalinedithiol)] (**1**), and its ester analogue. Electrochemical, spectroscopic and computational methods were used to understand the electronic characteristics of the complexes. In particular, this work demonstrates the first example of a Ni(II) complex that functions as a sensitiser in a dye-sensitised solar cell..

From the results obtained in solar testing we propose that our system is affected by dye-aggregation, with performance improving upon addition of cheno. In comparison with the analogous Pt(II) complex it is apparent that the limiting factor is the amount of photocurrent produced even after Cheno additives and TiCl₄ post-treatments ($I_{sc} = 0.293$ mA and 7.000 mA respectively). The satisfactory light harvesting, appropriate redox potentials and sufficient charge-separated lifetime suggest that the origin of the low photocurrents is the short lived excited state of the Ni(II) complex. This is also supported by the lack of emission observed upon photoexcitation. Although Ni complexes with long-lived excited states are uncommon, excited state lifetimes as long as 1-3 ns are known (Kuebler *et al.*, 1996), suggesting that higher-efficiency Ni-complex sensitisers are possible if this can be achieved in a complex also possessing the appropriate electrochemical and spectroscopic characteristics.

4. Experimental

The synthesis of 4,4'-Dicarboxy-2,2'-bipyridine (dcbpy), 4,4'-Di(CO₂Et)-2,2'-bipyridine (decby) and 2,3-quinoxalinedithiol (qdt) were carried out according to literature procedures (Hoertzl *et al.*, 2006; Dholakia *et al.*, 1958; Ghosh *et al.*, 1980; Theriot *et al.*, 1969). Ni(dcbpybpy)(qdt) and Ni(decby)(qdt) are novel complexes and have been synthesised using methods described below. 4,4'-Dimethyl-2,2'-Bipyridine (dmbpy), [Ni(H₂O)₆]Cl₂ and all other chemicals were purchased from Aldrich and used as received. Electrochemistry was carried out using a Pt working electrode, Pt rod counter electrode and Ag/AgCl reference electrode. All electrochemical experiments were carried out in DMF and the supporting electrolyte used was TBABF₄ (0.1M). After each experiment the reference electrode was calibrated against the ferrocene/ferrocenium couple which was found to be at 0.55 V.

The absorption spectra were recorded using a PerkinElmer Lambda 9 spectrophotometer controlled using the UV/Winlab software. Emission spectra were recorded at room temperature with 0.2mM ethanolic solutions, using a Fluoromax2 fluorimeter controlled by the ISAMain software. Density functional theory calculations were performed using the Gaussian 03 program (Frisch *et al.*, 2004) with the starting structure input using the builder program Arguslab. The Becke three parameters hybrid exchange and the Perdew–Wang 1991 correlation functionals (B3PW91) level of theory were used (Perdew *et al.*, 1993; Perdew *et al.*, 1996). Time-dependent density functional theory (TD-DFT) was performed in a DMF polarisable continuum model (Boes *et al.*, 2006), with the first 70 singlet transitions calculated.

To make the DSSCs, titanium dioxide paste (Dyesol, DSL-18NR-T) was deposited onto cleaned fluorine doped tin oxide conductive glass (TEC 8, Pilkington, UK) by doctor-blading. The film was dried at 100 °C for 15 min and then sintered at 450 °C for 30 min to remove the organics and to form a mesoporous film structure. The thickness of the film was approximately 12 µm. The films were sensitised with **1** using a solution of the dye in acetonitrile/*t*-butanol. The platinised counter electrode was fabricated following the previously reported procedure (Papageorgiou *et al.*, 1997).

The cell was completed by sealing the dye coated TiO₂ electrode and Pt electrode of a cell together by a thermal plastics spacer (Surlyn 1702, 25 µm, Solaronix) at 120 °C.

The electrolyte was introduced into the cell through the two holes which were drilled in the counter electrode. The holes were subsequently sealed using Kapton tape. The default electrolyte used was 4mM LiI, 3mM I₂, 1mM Guanidine thiocyanate, 5mM 4-tert-butylpyridine, 0.01M Valeronitrile in acetonitrile. The active area of the cell was 1 cm². The current-voltage characteristics of the cells were measured under simulated AM 1.5 illumination (100 mWcm⁻²) provided by a solar simulator (1 kW Xe with AM 1.5 filter, Müller) calibrated using a Digital Solar Power Meter. The Cheno additive was added dissolved in the dye baths at the same time as **1**.

The TiCl_4 post-treatment of the TiO_2 films was carried out prior to dye adsorption. The TiO_2 coated FTO cells were coated with a 40mM aqueous TiCl_4 solution and placed into a steam bath at 70°C for 30 min. The cells were removed, washed with deionised water, dried at 100°C for 15 min and then sintered at 500°C for 30 min. Dye adsorption was then carried out as described above.

4.1 Preparations

4.1.1 [Ni(dcbpy)(qdt)]: 1. $[\text{Ni}(\text{H}_2\text{O})_6]\text{Cl}_2$ (243.4 mg, 1.02 mmol) in 20 mL ethanol and dcbpy (252.7 mg, 1.04 mmol) in 6 mL ethanol with NaOH (100 mg, 2.50 mmol) were stirred for 1 min, before addition of qdt (201.7 mg, 1.05 mmol) in 5 mL ethanol with NaOH (84.39 mg, 2.11 mmol). The resulting purple reaction mixture yielded a red/purple precipitate which was collected by filtration. Yield = 54.3 %. δ_{H} (solvent, 250 MHz)/ppm: 7.45 (m, 2H-qdt), 7.70 (m, 2H, H-qdt), 7.95 (d, $J = 3.93$ Hz, 2H, H-bpy), 8.86 (d, $J = 4.83$ Hz, 2H, H-bpy), 8.99 (s, 2H, H-bpy). MS (positive ESI): m/z : 468 M^+ .

4.1.2 [Ni(decby)(qdt)]: 2. $[\text{Ni}(\text{H}_2\text{O})_6]\text{Cl}_2$ (48.5 mg, 0.20 mmol) in 5 mL ethanol and decby (61.8 mg, 0.21 mmol) in 6 mL DCM were stirred for 2 min before addition of qdt (39.2 mg, 0.20 mmol) in 5 mL ethanol and 5 mL aqueous sodium hydroxide (0.1M). The reaction was left to stir for 30 min, concentrated to a minimum volume and the product obtained as a solid precipitate by addition of excess ethanol. Precipitate was collected by centrifugation and washed with 10 mL ethanol. Yield = 35 %. δ_{H} (DMSO, 250 MHz)/ppm: 1.61 (b, 6H, $-\text{CH}_2-\text{CH}_3$), 4.65 (b, 4H, $-\text{CH}_2-\text{CH}_3$), 7.45 (b, 2H, H-qdt), 7.69 (b, 2H, H-qdt), 8.22 (b, 2H, H-bpy), 9.09 (b, 2H, H-bpy), 9.22 (b, 2H, H-bpy). MS (positive FAB); m/z : 551 M^+ . Elemental analysis: calculated for $\text{C}_{24}\text{H}_{28}\text{N}_4\text{O}_8\text{S}_2\text{Ni}$: C 42.24, H 4.53, N 9.00. Found: C 45.06, H 3.70, N 8.75

4.1.3 [Ni(decby)Cl₂]: 3 $[\text{Ni}(\text{H}_2\text{O})_6]\text{Cl}_2$ (100.8mg, 0.42 mmol) in 5 mL THF had a suspension of decby (76.9mg, 0.26 mmol) in THF (5ml) added over 3mins and the solution stirred for 2.5h. The precipitate was collected by filtration, washed with THF and dried. Yield: 117.0mg (64%). Found: C, 44.67; H, 3.82; N, 6.19. Calc. for $\text{C}_{16}\text{H}_{16}\text{O}_4\text{N}_2\text{NiCl}_2$: C, 44.73; H, 3.73; N, 6.52. +FAB-MS; m/z : 393 M^+ (-Cl).

References

- N. Alonso-Vante, J. F. Nierengarten, J. P. Sauvage, Spectral sensitisation of large-band-gap semiconductors (thin films and ceramics) by a carboxylated bis(1,10-phenanthroline)copper(I) complex, *Journal of the Chemical Society; Dalton Transactions*, (1994), pp.1649-1654.
- N. Armaroli, Photoactive mono- and polynuclear Cu(I)–phenanthrolines.
- A viable alternative to Ru(II)–polypyridines?, *Chemical Society Reviews*, (2001) 30, pp. 113-124.
- T. Bessho, E.C. Constable, M. Grätzel, A.H. Redondo, C.E. Housecroft, W. Kylberg, K. Nazeeruddin, M. Neuburger and S. Schaffner, An element of surprise-efficient copper-functionalised dye-sensitised solar cells, *Chemical Communications*, (2008), pp. 3717-3719.
- C.A. Bignozzi, R. Argazzi and C.J. Kleverlaan, Molecular and supramolecular sensitization of nanocrystalline wide band-gap semiconductors with mononuclear and polynuclear metal complexes, *Chemistry Society Review*, (2000), 29, pp. 87-96.
- E.S. Boes, P.R. Livotto and H. Stassen, Solvation of monovalent anions in acetonitrile and N,N-dimethylformamide: Parameterisation of the IEF-PCM model, *Chemical Physics*, (2006), 331, pp. 142–158.
- R. Chen, X. Yang, H. Tian, X.Wang, A. Hagfeldt and L. Sun, Effect of Tetrahydroquinoline Dyes Structure on the Performance of Organic Dye-Sensitised Solar Cells, *Chemistry of Materials*, (2007), 19, pp. 4007-4015.
- H. Choi, J.K. Lee, K.H. Song, K. Song, S.O. Kanga and J. Koa, Synthesis of new julolidine dyes having bithiophene derivatives for solar cell, *Tetrahedron*, (2007), 63, pp.1553–1559.
- E.C. Constable, A.H. Redondo, C.E. Housecroft, M. Neuburger and S. Schaffner Copper(I) complexes of 6,6'-disubstituted 2,2'-bipyridine dicarboxylic acids: new complexes for incorporation into copper-based dye sensitised solar cells (DSCs), *Dalton Transactions*, (2009), pp. 6634-6644.
- S. Dholakia, R.D. Gillard and F.L. Wimmer, 3,3'-Dicarbomethoxy-2,2'-Bipyridyl Complexes of Palladium(II), Platinum(II) and Rhodium(III), *Polyhedron*, (1958), 4, pp. 791-795.
- R. Eisenberg, D.G. Nocers, Overview of the Forum on Solar and Renewable Energy, *Inorganic Chemistry*, (2005), 44, pp. 6799-6801.
- S. Ferrere and B. Gregg, Photosensitisation of TiO₂ by [FeII(2,2'-bipyridine-4,4'-dicarboxylic acid)₂(CN)₂]: Band Selective Electron Injection from Ultra-Short-Lived Excited States, *Journal of the American Chemical Society*, (1998), 120, pp. 843-844.
- S. Ferrere, New Photosensitisers Based upon [Fe(L)₂(CN)₂] and [Fe(L)₃] (L) Substituted 2,2'-Bipyridine): Yields for the Photosensitisation of TiO₂ and Effects on the Band Selectivity, *Chemistry of Materials*, (2000), 12, pp. 1083-1089.

- S. Ferrere, New photosensitisers based upon $[\text{Fe}^{\text{II}}(\text{L})_2(\text{CN})_2]$ and $[\text{Fe}^{\text{II}}\text{L}_3]$, where L is substituted 2,2'-bipyridine, *Inorganica Chimica Acta*, (2002), pp. 329, 79–92.
- M.J. Frisch, G.W. Trucks, H.B. Schlegel, G.E. Scuseria, M.A. Robb, J.R. Cheeseman, J.A. Montgomery Jr., T. Vreven, K.N. Kudin, J.C. Burant, J.M. Millam, S.S. Iyengar, J. Tomasi, V. Barone, B. Mennucci, M. Cossi, G. Scalmani, N. Rega, G.A. Petersson, H. Nakatsuji, M. Hada, M. Ehara, K. Toyota, R. Fukuda, J. Hasegawa, M. Ishida, T. Nakajima, Y. Honda, O. Kitao, H. Nakai, M. Klene, X. Li, J. E. Knox, H.P. Hratchian, J.B. Cross, V. Bakken, C. Adamo, J. Jaramillo, R. Gomperts, R.E. Stratmann, O. Yazyev, A.J. Austin, R. Cammi, C. Pomelli, J.W. Ochterski, P.Y. Ayala, K. Morokuma, G.A. Voth, P. Salvador, J.J. Dannenberg, V.G. Zakrzewski, S. Dapprich, A.D. Daniels, M.C. Strain, O. Farkas, D.K. Malick, A.D. Rabuck, K. Raghavachari, J.B. Foresman, J.V. Ortiz, Q. Cui, A.G. Baboul, S. Clifford, J. Cioslowski, B.B. Stefanov, G. Liu, A. Liashenko, P. Piskorz, I. Komaromi, R.L. Martin, D.J. Fox, T. Keith, M.A. Al-Laham, C.Y. Peng, A. Nanayakkara, M. Challacombe, P.M.W. Gill, B. Johnson, W. Chen, M.W. Wong, C. Gonzalez and J.A. Pople, (2004), Gaussian 03, Revision C.02, Gaussian, Inc., Wallingford, CT.
- E.A.M. Geary, L.J. Yellowlees, L.A. Jack, I.D.H. Oswald, S. Parsons, N. Hirata, J.R. Durrant and N. Robertson, Synthesis, Structure, and Properties of $[\text{Pt}(\text{II})(\text{diimine})(\text{dithiolate})]$ Dyes with 3,3', 4,4', and 5,5'-Disubstituted Bipyridyl: Applications in Dye-Sensitised Solar Cells, *Inorganic Chemistry*, (2005), 44, pp. 242-250.
- P.K. Ghosh and T.G. Spiro, Photoelectrochemistry of Tris(bipyridyl)ruthenium(II) Covalently Attached to n-Type SnO_2 , *Journal of the American Chemical Society*, (1980), 102, pp. 5543-5549.
- B.A. Gregg, Interfacial processes in the dye-sensitized solar cell, *Coordination Chemistry Review*, (2004), 248, 1215.
- P.G. Hoertz, A. Staniszewski, A. Marton, G.T. Higgins, C.D. Incarvito, A.L. Rheingold and G.J. Meyer, Toward Exceeding the Shockley-Queisser Limit: Photoinduced Interfacial Charge Transfer Processes that Store Energy in Excess of the Equilibrated Excited State, *Journal of the American Chemical Society*, (2006), 128, pp. 8235.
- Islam, H. Sugihara, K. Hara, L. P. Singh, R. Katoh, M. Yanagida, Y. Takahashe, S. Murata and H. Arakawa, Dye Sensitisation of Nanocrystalline Titanium Dioxide with Square Planar Platinum(II) Diimine Dithiolate Complexes, *Inorganic Chemistry*, (2001), 40, pp. 5371-5380.
- S. Ito, P. Liska, P. Comte, R. Charvet, P. Péchy, U. Bach, L. Schmidt-Mende, S.M. Zakeeruddin, A. Kay, M.K. Nazeeruddin and M. Grätzel, Control of dark current in photoelectrochemical ($\text{TiO}_2/\text{I}^-/\text{I}_3^-$) and dye-sensitised solar cells *Chemical Communications*, (2005), pp. 4351-4353.
- S. Ito, H. Miura, S. Uchida, M. Takata, K. Sumioka, P. Liska, P. Comte, P. Péchy and M. Grätzel, High-conversion-efficiency organic dye-sensitised solar cells with a novel indoline dye, *Chemical Communications*, (2008), pp. 5194-5196.

- S.M. Kuebler and R.G. Denning, Population gratings in degenerate four-wave mixing studies of a nickel dithiolene at 1064 nm, *Chemical Physics Letters*, (1996), 250, pp. 120-127.
- K.L. McCall, J.R. Jennings, H. Wang, A. Morandeira, L.M. Peter, J.R. Durrant, L.J. Yellowlees, J.D. Woollins and N. Robertson, Novel ruthenium bipyridyl dyes with S-donor ligands and their application in dye-sensitised solar cells, *Journal of Photochemistry and Photobiology A: Chemistry*, (2009), 202, pp. 196–204.
- M. K. Nazeeruddin, A. Kay, I. Rodicio, R. Humphry-Baker, E. Mueller, P. Liska, N. Vlachopoulos, and M. Grätzel, Conversion of Light to Electricity by
- cis-X₂Bis(2,2'-bipyridyl-4,4'-dicarboxylate)ruthenium(II) Charge-Transfer Sensitisers (X = Cl⁻, Br⁻, I⁻, CN⁻, and SCN⁻) on Nanocrystalline TiO₂ Electrodes, *Journal of the American Chemical Society*, (1993), 115, pp. 6382-6390.
- O'Regan and M. Grätzel, A Low-Cost, High-Efficiency Solar Cell Based on Dye-Sensitised Colloidal TiO₂ Films, *Nature*, (1991), 353, pp. 737-740.
- N. Papageorgiou, W.F. Maier and M. Grätzel, An Iodine/Triiodide Reduction Electrocatalyst for Aqueous and Organic Media, *Journal of the Electrochemical Society*, (1997), 144, pp. 876–884.
- J.P. Perdew, J.A. Chevary, S.H. Vosko, K.A. Jackson, M.R. Pederson, D.J. Singh and C. Fiolhais, Applications of the Generalised Gradient Approximation for Exchange and Correlation, *Physical Review B*, (1993), 48, pp. 4978–14978.
- J.P. Perdew, K. Burke and Y. Wang, Generalised gradient approximation for the exchange-correlation hole of a many-electron system, *Physical Review B*, (1996), 54, pp. 16533–16539.
- N. Robertson, Optimizing Dyes for Dye-Sensitized Solar Cells, *Angewandte Chemie International Edition*, (2006), 45, pp. 2338-2345.
- N. Robertson, Cu(I) versus Ru(II): Dye-Sensitised Solar Cells and Beyond, *Chemistry and Sustainability*, 2008, pp. 977-979.
- S. Sakai, T. Kuroki and T. Hamada, Synthesis of a new copper(I) complex, [Cu(tmdbpy)₂]⁺ (tmdbpy = 4,4',6,6'-tetramethyl-2,2'-bipyridine-5,5'-dicarboxylic acid), and its application to solar cells, *Journal of the Chemical Society; Dalton Transactions*, (2002), pp. 840-842.
- K. Sayama, S. Tsukagoshi, T. Mori, K. Hara, Y. Ohga, A. Shinpou, Y. Abe, S. Suga and H. Arakawa, Efficient sensitisation of nanocrystalline TiO₂ films with cyanine and merocyanine organic dyes, *Solar Energy Materials and Solar Cells*, (2003), 80, pp. 47–71.
- P.M. Sommeling, B.C. O'Regan, R.R. Haswell, H.J.P. Smit, N.J. Bakker, J.J.T. Smits, J.M. Kroon and J.A.M. van Roosmalen, Influence of a TiCl₄ Post-Treatment on Nanocrystalline TiO₂ Films in Dye-Sensitised Solar Cells, *Journal of Physical Chemistry B*, (2006), 110, pp. 19191-19197.
- L.J. Theriot, K.K. Ganguli, S. Kavarnos and I. Bernal, Metal Complexes of 2,3-Quinoxalinedithiol, *Journal of Inorganic and Nuclear Chemistry*, (1969), 31, pp. 3133-3140.

- J.H. Yum, S. Moon, R. Humphry-Baker, P. Walter, T. Geiger, F. Nüesch, M. Grätzel and M.K. Nazeeruddin, Effect of coadsorbent on the photovoltaic performance of squaraine sensitised nanocrystalline solar cells, *Nanotechnology*, (2008), 19, pp. 424005.
- S.M. Zakeeruddin, M.K. Nazeeruddin, P. Pechy, F.P. Rotzinger, R. Humphry-Baker, K. Kalyanasundaram and M. Grätzel, Molecular Engineering of Photosensitizers for Nanocrystalline Solar Cells: Synthesis and Characterization of Ru Dyes Based on Phosphonated Terpyridines *Inorganic Chemistry*, (1997), 36, pp. 5937.
- K. Zweibel, Harnessing Solar Power: The Photovoltaics Challenge, *American Journal of Physics*, (1993), 61, pp. 286.